

# Adversarial Balancing-based Representation Learning for Causal Effect Inference with Observational Data

Xin Du

Technische Universiteit Eindhoven  
x.du@tue.nl

Lei Sun

University at Buffalo  
leisun@buffalo.edu

Wouter Duivesteijn

Technische Universiteit Eindhoven  
w.duivesteijn@tue.nl

Alexander Nikolaev

University at Buffalo  
anikolae@buffalo.edu

Mykola Pechenizkiy

Technische Universiteit Eindhoven  
m.pechenizkiy@tue.nl

July 5, 2022

## Abstract

Learning causal effects from observational data greatly benefits a variety of domains such as health care, education and sociology. For instance, one could estimate the impact of a new drug to improve the survive rate. In this paper, we conduct causal inference with observational studies based on potential outcome framework (PO) (Rubin, 2005). The central problem for causal effect inference in PO is dealing with the unobserved counterfactuals and treatment selection bias. The state-of-the-art approaches focus on solving these problems by balancing the treatment and control groups (Sun and Nikolaev, 2016). However, during the learning and balancing process, highly predictive information from the original covariate space might be lost. In order to build more robust estimators, we tackle this information loss problem by presenting a method called **Adversarial Balancing-based representation learning for Causal Effect Inference (ABCEI)**, based on the recent advances in representation learning. ABCEI uses adversarial learning to balance the distributions of treatment and control group in the latent representation space, without any assumption on the form of the treatment selection/assignment function. ABCEI preserves useful information for predicting causal effects under the regularization of a mutual information estimator. The experimental results show that ABCEI is robust against treatment selection bias, and matches/outperforms the

state-of-the-art approaches. Our experiments show promising results on several datasets, representing different health care domains among others.

## 1 Introduction

Many domains of science require inference of causal effects, including health-care (Casucci et al., 2017), economics and marketing (LaLonde, 1986; Smith and Todd, 2005), sociology (Morgan and Harding, 2006) and education (Zhao and Heffernan, 2017). For instance, medical scientists must know whether a new medicine is more beneficial for patients; teachers want to know if the teaching plan can be beneficial for students; economists need to evaluate how a policy affects the unemployment rates. Properly estimating causal effects is an important task for machine learning research.

Conducting Randomized Controlled Trials (RCT) can be time-consuming, expensive, or unethical (e.g. for studying the effect of smoking). Hence, approaches for causal inference from observational data are needed. The core issue of causal effect inference from observational data is confounding: variables might affect both intervention and treatment outcomes. For example, patients with more personal wealth are in a better position to get new medicines, increasing the likelihood that they survive. Inferring causal effect without controlling for confounders will lead to errors. Throughout this paper, we assume that all the variables in the causal system can be observed and measured, so that the causal effects we are interested can be identifiable from the observational data (Pearl, 2009).

Under potential outcome framework, people usually focus on matching / balancing covariates according to confounders, e.g. based on mutual information (Sun and Nikolaev, 2016) or propensity scores (Dehejia and Wahba, 2002). Average Treatment Effect (ATE) or Average Treatment effect on the Treated (ATT) can be properly estimated after those steps. To account for heterogeneity in subpopulations (Pearl, 2017; Bertsimas et al., 2018), articles about Conditional Average Treatment Effects (CATE) have come out recently (Shalit et al., 2017; Lu et al., 2018). CATE can be estimated by regressing the difference of Individual Treatment Effects (ITEs), which cannot be directly observed from the data, because of the unobservable counterfactuals (Künzel et al., 2019). The main challenges for CATE estimation are two-fold: on the one hand, in observational data, we only know the factual outcome of each unit (treated or untreated), but we will never know the counterfactual outcome; on the other hand, usually the distributions of covariates in treatment and control group are unbalanced (*treatment selection bias*). If we directly employ the standard supervised learning framework to learn the treatment outcome, we will get a biased model suffering from generalization error (Swaminathan and Joachims, 2015b).

To overcome these challenges, we propose a unified framework to encode the input covariates into a latent representation space, and estimate the treatment outcomes with those representations. There are three components on

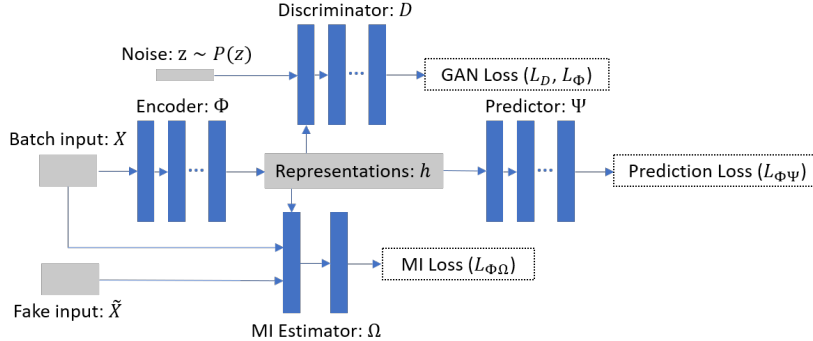


Figure 1: Deep neural network architecture of ABCEI for causal effect inference.

top of the encoder in our model: (1) **mutual information estimation**: an estimator is specified to estimate and maximize the mutual information between representations and covariates; (2) **adversarial balancing**: the encoder plays an adversarial game with a discriminator, trying to fool the discriminator by minimizing the discrepancies between distributions of representations from the treatment and control group; (3) **treatment outcome prediction**: a predictor over latent space is employed to estimate the treatment outcomes. By jointly optimizing the three components via back propagation, we can get a robust estimator on causal effects. The overarching architecture of our framework is shown in Figure 1. As a summary, our main contributions are:

1. We propose a novel model: **Adversarial Balancing**-based representation learning for **Causal Effect Inference (ABCEI)** with observational data. ABCEI addresses information loss and selection bias by learning highly informative and balanced representations in latent space.
2. A neural network encoder is constrained by a mutual information estimator to minimize the information loss between representations and the input covariates, which preserves highly predictive information for causal effect inference.
3. We employ an adversarial learning method to balance representations between treatment and control groups, which deals with the selection bias problem without any assumption on the form of the treatment selection function, unlike, e.g., the propensity score method.
4. We conduct various experiments on synthetic and real-world datasets. ABCEI outperforms most of the state-of-the-art methods on benchmark datasets. We show that ABCEI is robust against different experimental settings. By supporting mini-batch, ABCEI can be applied on large-scale datasets.

## 2 Preliminaries

In order to properly handle treatment selection bias and counterfactuals, causal effect estimation must solve two central problems: balancing covariates and specifying the outcome model. Recent methods in causal inference tackle one or both of these problems. (Yao et al., 2018) propose to use hard samples, to preserve local similarity information from covariate space to latent representation space. The hard sample mining process is highly dependent on the propensity score model, which is not robust when the propensity score model is misspecified. (Imai and Ratkovic, 2014; Ning et al., 2018) propose estimators which are robust even when the propensity score model is not correctly specified. (Kallus, 2018a,b; Ozery-Flato et al., 2018) propose to generate balanced weights for data samples to minimize a selected imbalance measure in covariate space. (Shalit et al., 2017) propose to derive upper bounds on the estimation error by considering both covariate balancing and potential outcomes. Highly predictive information might be lost in the reweighing or balancing processes of these methods.

To address these problems, we propose a framework (cf. Figure 1), which generates balanced representations preserving highly predictive information in latent space without considering propensity scores. We design a two-player adversarial game, between an encoder that transforms covariates to latent representations and a discriminator which distinguishes representations from control and treatment group. Unlike in the classical GAN framework, here, the ‘true distribution’ (latent representations of the control group<sup>1</sup>) in this game also must be generated by the encoder. On the other hand, to prevent losing useful information during the balancing process, we use a mutual information estimator to constrain the encoder to preserve highly predictive information (Hjelm et al., 2018). The outcome data are also considered in this unified framework to specify the causal effect predictor.

### 2.1 Problem Setup

Assume an observational dataset  $\{X, T, Y\}$ , with covariate matrix  $X \in \mathbb{R}^{n \times k}$ , binary treatment vector  $T \in \{0, 1\}^n$ , and treatment outcome vector  $Y \in \mathbb{R}^n$ . Here,  $n$  denotes the number of observed units, and  $k$  denotes the number of covariates in the dataset. For each unit  $u$ , we have  $k$  covariates  $x_1, \dots, x_k$ , associated with one treatment variable  $t \in \{0, 1\}$  and one treatment outcome  $y$ . According to the Rubin-Neyman causal model (Rubin, 2005), two potential outcomes  $y_0, y_1$  exist for treatments  $\{0, 1\}$ , respectively. We call  $y_t$  the *factual outcome*, denoted by  $y_f$ , and  $y_{1-t}$  the *counterfactual outcome*, denoted by  $y_{cf}$ . Assuming there is a joint distribution  $P(x, t, y_0, y_1)$ , we make the following assumptions:

**Assumption 1** *Conditioned on  $x$ , the potential outcomes  $y_0, y_1$  are independent of  $t$ , which can be stated as:  $(y_0, y_1) \perp\!\!\!\perp t|x$ .*

<sup>1</sup>our method supports representations of either treatment/control group or both as ‘true distribution’.

**Assumption 2** For all sets of covariates and for all treatments, the probability of treatment assignment will always be strictly larger than 0 and strictly smaller than 1, which can be expressed as:  $0 < P(t|x) < 1, \forall t$  and  $\forall x$ .

Assumption 1 indicates that all the confounders are observed, i.e., *no unmeasured confounder is present*. Assumption 2 allows us to estimate the CATE for any  $x$  in the covariate space. Under these assumptions, we can formalize the definition of CATE (Shalit et al., 2017) for our task:

**Definition 1** The Conditional Average Treatment Effect (CATE), for unit  $u$  is:  $CATE(u) := \mathbb{E}[y_1 | x^u] - \mathbb{E}[y_0 | x^u]$ .

We can now define the Average Treatment Effect (ATE) and the Average Treatment effect on the Treated (ATT) as:

$$ATE := \mathbb{E}[CATE(u)] \quad ATT := \mathbb{E}[CATE(u) | t = 1].$$

Because the joint distribution  $P(x, t, y_0, y_1)$  is unknown, we can only try to estimate  $CATE(u)$  from observational data. A function over the covariate space  $\mathcal{X}$  can be defined as  $f : \mathcal{X} \times \{0, 1\} \rightarrow \mathcal{Y}$ . The estimate of  $CATE(u)$  can now be defined:

**Definition 2** Given an observational dataset  $\{X, T, Y\}$  and a function  $f$ , for unit  $u$ , the estimate of  $CATE(u)$  is:

$$\widehat{CATE}(u) = f(x^u, 1) - f(x^u, 0).$$

In order to properly accomplish the task of CATE estimation, we need to find an optimal function over the covariate space for both systems ( $t = 1$  and  $t = 0$ ).

### 3 Proposed Method

In order to overcome the challenges in CATE estimation, we build our model on recent advances in representation learning. We propose to define a function  $\Phi : \mathcal{X} \rightarrow \mathcal{H}$ , and a function  $\Psi : \mathcal{H} \rightarrow \mathcal{Y}$ . Then we have  $\widehat{Y}_T = f(X, T) = \Psi(\Phi(X), T) = \Psi(h, T)$ . Instead of directly estimating the treatment outcome conditioned on covariates, we firstly use an encoder to learn latent representations of covariates. We simultaneously learn latent representations and estimate the treatment outcome. However, the function  $f$  would still suffer from information loss and treatment selection bias, unless we constrain the encoder  $\Phi$  to learn balanced representations while preserving useful information.

#### 3.1 Mutual Information Estimation

Consider the information loss when transforming covariates into latent space. The non-linear statistical dependencies between variables can be acquired by mutual

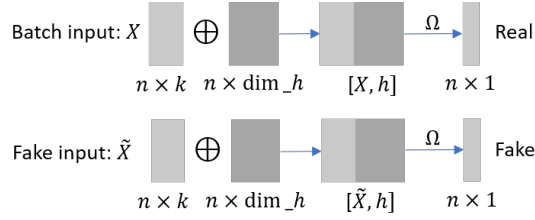


Figure 2: MI estimator between covariates and latent representations.

information (MI) (Kinney and Atwal, 2014). Thus we use MI between latent representations and original covariates as a measure to account for information loss:

$$I(X; h) = \int_{\mathcal{X}} \int_{\mathcal{H}} P(x, h) \log \left( \frac{P(x, h)}{P(x)P(h)} \right) dh dx.$$

We denote the joint distribution between covariates and representations by  $\mathbb{P}_{Xh}$  and the product of marginals by  $\mathbb{P}_X \otimes \mathbb{P}_h$ . From the viewpoint of Shannon information theory, mutual information can be represented as Kullback-Leibler (KL) divergence:

$$I(X; h) := H(X) - H(X|h) := D_{KL}(\mathbb{P}_{Xh} || \mathbb{P}_X \otimes \mathbb{P}_h),$$

It is hard to compute MI in continuous and high-dimensional spaces, but one can capture a lower bound of MI with the Donsker-Varadhan representation of KL-divergence (Donsker and Varadhan, 1983):

**Theorem 1 (Donsker-Varadhan)**

$$D_{KL}(\mathbb{P}_{Xh} || \mathbb{P}_X \otimes \mathbb{P}_h) = \sup_{\Omega \in \mathcal{C}} \mathbb{E}_{\mathbb{P}_{Xh}} [\Omega(x, h)] - \log \mathbb{E}_{\mathbb{P}_X \otimes \mathbb{P}_h} \left[ e^{\Omega(x, h)} \right].$$

Here,  $\mathcal{C}$  denotes the set of unconstrained functions  $\Omega$  (detailed proof is in the supplementary material). Inspired by Mutual Information Neural Estimation (MINE) (Belghazi et al., 2018), we propose to establish a neural network estimator for MI. Specifically, let  $\Omega$  be a function:  $\mathcal{X} \times \mathcal{H} \rightarrow \mathbb{R}$  parametrized by a deep neural network, we have:

$$\begin{aligned} I(X; h) &:= D_{KL}(\mathbb{P}_{Xh} || \mathbb{P}_X \otimes \mathbb{P}_h) \geq \hat{I}_{\Omega}(X; h) \\ &:= \mathbb{E}_{\mathbb{P}_{Xh}} [\Omega(x, h)] - \log \mathbb{E}_{\mathbb{P}_X \otimes \mathbb{P}_h} \left[ e^{\Omega(x, h)} \right]. \end{aligned} \tag{1}$$

By distinguishing the joint distribution and the product of marginals, the estimator  $\Omega$  approximates the MI with arbitrary precision. In practice, as shown in Figure 2, we concatenate the input covariates  $X$  with representations  $h$  one by one to create positive samples (as samples from the true joint distribution). Then, we randomly shuffle  $X$  on the batch axis to create fake input covariates  $\tilde{X}$ . Representations  $h$  are concatenated with fake input  $\tilde{X}$  to create negative

samples (as samples from the product of marginals). From Equation (1) we can derive the loss function for the MI estimator:

$$L_{\Phi\Omega} = -\mathbb{E}_{x\sim X} [\Omega(x, h)] + \log \mathbb{E}_{x\sim \bar{X}} [e^{\Omega(x, h)}].$$

Information loss can be diminished by simultaneously optimizing the encoder  $\Phi$  and the MI estimator  $\Omega$  to minimize  $L_{\Phi\Omega}$  iteratively via gradient descent.

### 3.2 Adversarial Balancing

The representations of treatment and control groups are denoted by  $h(t=1)$  and  $h(t=0)$ , corresponding to the input covariate groups  $X(t=1)$  and  $X(t=0)$ . The discrepancy between distributions of the treatment and control groups is an urgent problem in need of a solution. To decrease this discrepancy, we propose an adversarial learning method to constrain the encoder to learn treatment and control representations that are balanced distributions. We build an adversarial game between a discriminator  $D$  and the encoder  $\Phi$ , inspired by the framework of Generative Adversarial Networks (GAN) (Goodfellow et al., 2014). In the classical GAN framework, a source of noise is mapped to a generated image by a generator. A discriminator is trained to distinguish whether an input sample is from true or synthetic image distribution generated by the generator. The aim of classical GAN is training a reliable discriminator to distinguish fake and real images, and using the discriminator to train a generator to generate images by fooling the discriminator.

In our adversarial game: (1) we draw a noise vector  $z \sim P(z)$  which has the same length as the latent representations, where  $P(z)$  can be a spherical Gaussian distribution or a Uniform distribution; (2) we separate representation by treatment assignment, and form two distributions:  $P_{h(t=1)}$  and  $P_{h(t=0)}$ ; (3) we train a discriminator  $D$  to distinguish concatenated vectors from treatment and control group ( $[z, h(t=1)]$  and  $[z, h(t=0)]$ ); (4) we optimize the encoder  $\Phi$  to generate balanced representations to fool the discriminator.

According to the architecture of ABCEI, the encoder is associated with the MI estimator  $\Omega$ , treatment outcome predictor  $\Psi$  and adversarial discriminator  $D$ . This means that the training process is iteratively adjusting each of the components. The instability of GAN training will become serious in this context. To stabilize the training of GAN, we propose to use the framework of Wasserstein GAN with gradient penalty (Gulrajani et al., 2017). By removing the sigmoid layer and applying the gradient penalty to the data between the distributions of treatment and control groups, we can find a function  $D$  which satisfies the 1-Lipschitz inequality:

$$\|D(x^1) - D(x^2)\| \leq \|x^1 - x^2\|.$$

We can write down the form of our adversarial game:

$$\min_{\Phi} \max_D \mathbb{E}_{h\sim P_{h(t=0)}} [D([z, h])] - \mathbb{E}_{h\sim P_{h(t=1)}} [D([z, h])] - \beta \mathbb{E}_{h\sim P_{\text{penalty}}} [(\|\nabla_{[z, h]} D([z, h])\|_2 - 1)^2],$$

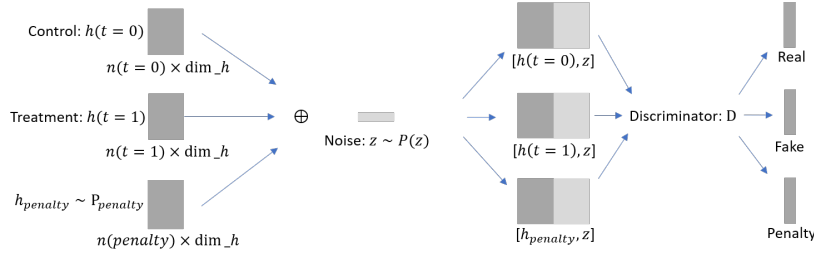


Figure 3: Adversarial learning structure for representation balancing.

where  $P_{\text{penalty}}$  is the distribution acquired by uniformly sampling along the straight lines between pairs of samples from  $P_{h(t=0)}$  and  $P_{h(t=1)}$ . The adversarial learning process is in Figure 3.

This ensures the encoder  $\Phi$  to be smoothly trained to generate balanced representations. We can write down the training objective for discriminator and encoder, respectively:

$$\begin{aligned}
 L_D &= -\mathbb{E}_{h \sim P_{h(t=0)}} [D([z, h])] + \mathbb{E}_{h \sim P_{h(t=1)}} [D([z, h])] \\
 &\quad + \beta \mathbb{E}_{h \sim P_{\text{penalty}}} [(\|\nabla_{[z, h]} D([z, h])\|_2 - 1)^2], \\
 L_\Phi &= \mathbb{E}_{h \sim P_{h(t=0)}} [D([z, h])] - \mathbb{E}_{h \sim P_{h(t=1)}} [D([z, h])].
 \end{aligned}$$

### 3.3 Treatment Outcome Prediction

The final step for CATE estimation is to predict the treatment outcomes with learned representations. We establish a neural network predictor, which takes latent representations and treatment assignments of units as the input, to conduct outcome prediction:  $\hat{y}_t = \Psi(h, t)$ . We can write down the loss function of the training objective as:

$$L_{\Phi\Psi} = \mathbb{E}_{(h, t, y_t) \sim \{h, T, Y_T\}} [(\Psi(h, t) - y_t)^2] + \lambda R(\Psi).$$

Here,  $R$  is a regularization on  $\Psi$  for the model complexity.

### 3.4 Learning Optimization

W.r.t. the architecture in Figure 1, we minimize  $L_{\Phi\Omega}$ ,  $L_\Phi$ , and  $L_{\Phi\Psi}$ , respectively, to iteratively optimize parameters in the global model. The optimization steps are handled with the stochastic method Adam (Kingma and Ba, 2014), training the model within Algorithm 1. Optimization details and computational complexity analysis are given in the supplementary material.



---

**Algorithm 1** ABCEI

---

Input: Observational dataset  $\{X, T, Y\}$ ; loss function  $L_{\Phi\Omega}$ ,  $L_{\Phi}$  and  $L_{\Phi\Psi}$ ,  $L_D$ ;  
Neural Networks  $\Phi$ ,  $\Omega$ ,  $D$ ,  $\Psi$ ; parameters  $\Theta_{\Phi}$ ,  $\Theta_{\Omega}$ ,  $\Theta_D$ ,  $\Theta_{\Psi}$

**repeat**

- Draw mini-batch  $\{X_b, T_b, Y_b\} \subset \{X, T, Y\}$
- Compute representations  $h = \Phi(X_b)$
- Draw fake input  $\tilde{X}_b \sim \tilde{\mathbb{P}}$
- Draw noise  $z \sim \mathcal{N}(0, I)$
- Set  $\Theta_{\Phi}$ ,  $\Theta_{\Omega} \leftarrow \text{Adam}(L_{\Phi\Omega}(X_b, \tilde{X}_b, h), \Theta_{\Phi}, \Theta_{\Omega})$
- for**  $i = 1$  to 3 **do**

  - Set  $\Theta_D \leftarrow \text{Adam}(L_D(h, z, T_b), \Theta_D)$
  - Set  $\Theta_{\Phi} \leftarrow \text{Adam}(L_{\Phi}(h, z, T_b), \Theta_{\Phi})$
  - Set  $\Theta_{\Phi}$ ,  $\Theta_{\Psi} \leftarrow \text{Adam}(L_{\Phi\Psi}(h, T_b, Y_b), \Theta_{\Phi}, \Theta_{\Psi})$

**until** convergence

---

## 4 Experiments

There are two ways to validate and test the performance of causal inference methods: the one is to use simulated or semi-simulated treatment outcomes, e.g., dataset IHDP (Hill, 2011); the other is to use RCT datasets and add a non-randomized component to generate imbalanced datasets, e.g., dataset Jobs (LaLonde, 1986; Smith and Todd, 2005). We designed experiments along both paths for evaluating our method. The four benchmark datasets IHDP, Jobs, Twins (Louizos et al., 2017) and ACIC (Dorie et al., 2019) are used. For IHDP, Jobs, Twins and ACIC, the experimental results are averaged over 1000, 100, 100, 7700 train/validation/test sets respectively with split sizes 60%/30%/10%. Datasets description and evaluation metrics are given in the supplementary material.

### 4.1 Details of Datasets

**IHDP** The *Infant Health and Development Program* (IHDP) studies the impact of specialist home visits on future cognitive test scores. Covariates in the semi-simulated dataset are collected from a real-world randomized experiment. The treatment selection bias is created by removing a subset of the treatment group. We use the setting ‘A’ in (Dorie, 2016) to simulate treatment outcomes. This dataset includes 747 units (608 control and 139 treated) with 25 covariates associated with each unit.

**Jobs** The *Jobs* dataset (LaLonde, 1986; Smith and Todd, 2005) studies the effect of job training on the employment status. It consists of a non-randomized component from observational studies and a randomized component based on the National Supported Work program. The randomized component includes 722

units (425 control and 297 treated) with seven covariates, and the non-randomized component (PSID comparison group) includes 2490 control units.

**Twins** The *Twins* dataset is created based on the “Linked Birth / Infant Death Cohort Data” by NBER <sup>2</sup>. Inspired by (Almond et al., 2005), we employ a matching algorithm to select twin births in the USA between 1989-1991. By doing this, we get units associated with 43 covariates including education, age, race of parents, birth place, marital status of mother, the month in which pregnancy prenatal care began, total number of prenatal visits and other variables indicating demographic and health conditions. We only select twins that have the same gender who both weigh less than 2000g. For the treatment variable, we use  $t = 0$  indicating the lighter twin and  $t = 1$  indicating the heavier twin. We take the mortality of each twin in their first year of life as the treatment outcome, inspired by (Louizos et al., 2017). Finally, we have a dataset consisting of 12,828 pairs of twins whose mortality rate is 19.02% for the lighter twin and 16.54% for the heavier twin. Hence, we have observational treatment outcomes for both treatments. In order to simulate the selection bias, we selectively choose one of the twins to observe with regard to the covariates associated with each unit as follows:  $t|x \sim \text{Bernoulli}(\sigma(w^T x + n))$ , where  $w^T \sim \mathcal{N}(0, 0.1 \cdot I)$  and  $n \sim \mathcal{N}(1, 0.1)$ .

**ACIC** The *Atlantic Causal Inference Conference* (ACIC) (Dorie et al., 2019) is derived from real-world data with 4802 observations using 58 covariates. There are 77 datasets which are simulated with different treatment selection and outcome functions. Each dataset is generated with 100 random replications independently. In this benchmark, different settings like degrees of non-linearity, treatment selection bias and magnitude of treatment outcome are considered.

## 4.2 Evaluation Metrics

Since the ground truth CATE for the IHDP dataset is known, we can employ Precision in Estimation of Heterogeneous Effect (PEHE) (Hill, 2011), as the evaluation metric of CATE estimation:

$$\epsilon_{PEHE} = \frac{1}{n} \sum_{u=1}^n ((\mathbb{E}[y_1|x^u] - \mathbb{E}[y_0|x^u]) - (f(x^u, 1) - f(x^u, 0)))^2.$$

Subsequently, we can evaluate the precision of ATE estimation based on estimated CATE. For the Jobs dataset, because we only know parts of the ground truth (the randomized component), we cannot evaluate the performance of ATE estimation. Following (Shalit et al., 2017), we evaluate the precision of ATT estimation and policy risk estimation, where

$$R_{pol}(\pi) = 1 - [\mathbb{E}(y_1|\pi(x^u) = 1) \cdot P(\pi = 1) + \mathbb{E}(y_0|\pi(x^u) = 0) \cdot P(\pi = 0)].$$

<sup>2</sup><https://nber.org/data/linked-birth-infant-death-data-vital-statistics-data.html>

In this paper, we consider  $\pi(x^u) = 1$  when  $f(x^u, 1) - f(x^u, 0) > 0$ . For the Twins dataset, because we only know the observed treatment outcome for each unit, we follow (Louizos et al., 2017) using area under ROC curve (AUC) as the evaluation metric. For ACIC dataset, we follow (Ozery-Flato et al., 2018) to use RMSE ATE as performance metric.

### 4.3 Baseline Methods

We compare with the following baselines: least square regression using treatment as a feature (**OLS/LR<sub>1</sub>**); separate least square regressions for each treatment (**OLS/LR<sub>2</sub>**); balancing linear regression (**BLR**) and balancing neural network (**BNN**) (Johansson et al., 2016);  $k$ -nearest neighbor (**k-NN**) (Crump et al., 2008); Bayesian additive regression trees (**BART**) (Sparapani et al., 2016); random forests (**RF**) (Breiman, 2001); causal forests (**CF**) (Wager and Athey, 2017); treatment-agnostic representation networks (**TARNet**) and counterfactual regression with Wasserstein distance (**CFR-Wass**) (Shalit et al., 2017); causal effect variational autoencoders (**CEVAE**) (Louizos et al., 2017); local similarity preserved individual treatment effect (**SITE**) (Yao et al., 2018). MMD measure using RBF kernel (**MMD-V1**, **MMD-V2**) (Kallus, 2018b,a). Adversarial balancing with cross-validation procedure (**ADV-LR/SVM/MLP**) (Ozery-Flato et al., 2018). We show the quantitative comparison between our method and the state-of-the-art baselines. Experimental results (in-sample and out-of-sample) on IHDP, Jobs and Twins datasets are reported. Specifically, we use ABCEI\* to represent our model without the mutual information estimation component, and ABCEI\*\* to represent our model without the adversarial learning component.

### 4.4 Results

Experimental results are shown in Tables 1 and 2. It would be unsound to report statistical test results over the results reported in these tables; due to varying (un-)availability of ground truth, we must resort to reporting varying evaluation measures per dataset, over which it would not be appropriate to aggregate in a single statistical hypothesis test. However, one can see that ABCEI performs best in ten out of twelve cases, not only by the best number in the column, but often also by a non-overlapping empirical confidence interval with that of the best competitor (cf. reported standard deviations). This provides evidence that ABCEI is a substantial improvement over the state of the art.

Due to the existence of treatment selection bias, regression based methods suffer from high generalization error. Nearest neighbor based methods consider unit similarity to overcome selection bias, but cannot achieve balance globally. Recent advances in representation learning bring improvements in causal effect estimation. Unlike CFR-Wass, BNN, and SITE, ABCEI considers information loss and balancing problems. The mutual information estimator ensures that the encoder learns representations preserving useful information from the original covariate space. The adversarial learning component constrains the encoder to learn balanced representations. This causes ABCEI to achieve better performance

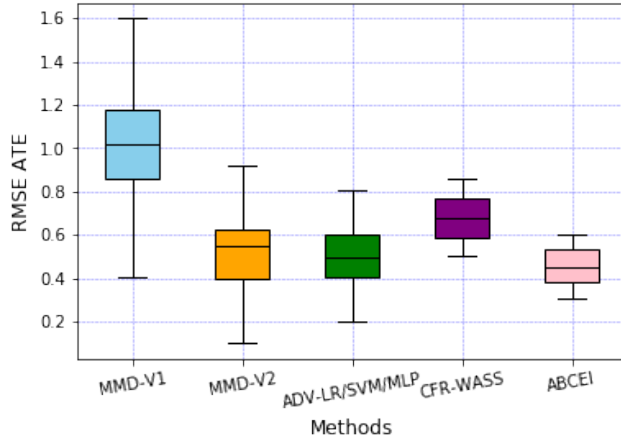


Figure 4: Results on ACIC datasets.

than the baselines. We also report the performance of our model without mutual information estimator or adversarial learning, respectively, as ABCEI\*, ABCEI\*\*. From the results we can see that performance suffers when either of these components is left out, which demonstrates the importance of combining adversarial learning and mutual information estimation in ABCEI.

In Figure 4, we compare ABCEI with recent balancing methods on ACIC benchmark. As we can see, the variance of representation learning methods are lower than methods reweighing samples on covariate space. We also found that the adversarial balancing methods perform better on ATE estimation. ABCEI has the advantage of adversarial balancing as well as preserving predictive information in latent space, which makes it outperforms the other baselines.

#### 4.5 Robustness Analysis on Selection Bias

To investigate the performance of our model when varying the level of selection bias, we generate toy datasets by varying the discrepancy between the treatment and control groups. We draw 8000 samples with ten covariates  $x \sim \mathcal{N}(\mu_0, 0.5 \cdot (\Sigma + \Sigma^T))$  as control group, where  $\Sigma \sim \mathcal{U}((-1, 1)^{10 \times 10})$ . Then we draw 2000 samples from  $x \sim \mathcal{N}(\mu_1, 0.5 \cdot (\Sigma + \Sigma^T))$ . By adjusting  $\mu_1$ , we generate treatment groups with varying selection bias, which can be measured by KL-divergence. For the outcomes, we generate  $y|x \sim (w^T x + n)$ , where  $n \sim \mathcal{N}(0^{2 \times 1}, 0.1 \cdot I^{2 \times 2})$  and  $w \sim \mathcal{U}((-1, 1)^{10 \times 2})$ .

In Figure 5, we can see the robustness of ABCEI, in comparison with CFR-Wass, BART, and SITE. The reported experimental results are averaged over 100 test sets. From the figure, we can see that with increasing KL-divergence, our method achieves more stable performance. We do not visualize standard deviations as they are negligibly small.

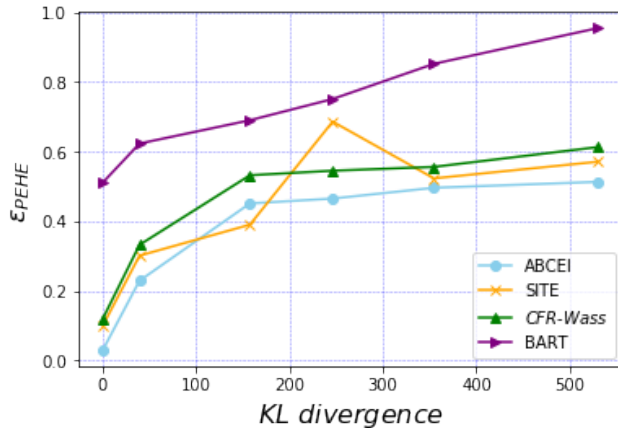


Figure 5:  $\epsilon_{PEHE}$  on datasets with varying treatment selection bias. ABCEI is comparatively robust.

#### 4.6 Robustness Analysis on Mutual Information Estimation

To investigate the impact of minimizing the information loss on causal effect learning, we block the adversarial learning component and train our model on the IHDP dataset. We record the values of the estimated MI and  $\epsilon_{PEHE}$  in each epoch. In Figure 6, we report the experimental results averaged over 1000 test sets. We can see that with increasing MI, the mean square error decreases and reaches a stable region. But without the adversarial balancing component, the  $\epsilon_{PEHE}$  cannot be further lowered due to the selection bias. This result indicates that even though the estimators benefit from highly predictive information, they will still suffer if imbalance is ignored.

#### 4.7 Balancing Performance of Adversarial Learning

In Figure 7, we visualize the learned representations on the IHDP and Jobs datasets using t-SNE. We can see that compared to CFR-Wass, the coverage of the treatment group over the control group in the representation space learned by our method is better. This showcases the degree to which adversarial balancing improves the performance of ABCEI, especially in population causal effect (ATE, ATT) inference.

## 5 Related Work

Work on causality learning falls into two categories: causal inference and causal discovery (Mooij et al., 2016). In the branch of causal inference, three kinds of data are used: data from Randomized Controlled Trials (RCT), observational

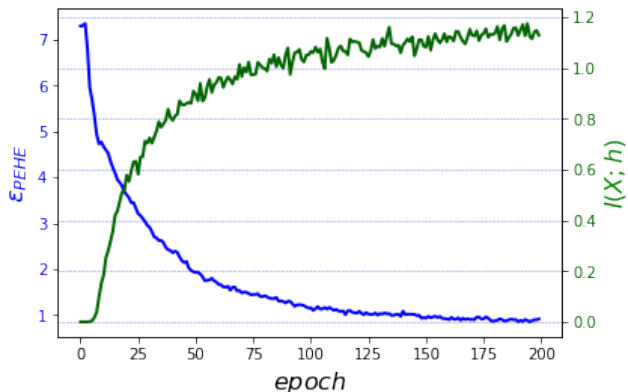


Figure 6: Mutual information (MI) between representations and original covariates, as well as  $\epsilon_{PEHE}$  in each epoch. With increasing MI,  $\epsilon_{PEHE}$  decreases.

data for which all the (potential) confounders can be observed, and observational data with unobserved confounders. A branch of research with RCT datasets focuses on identification of heterogeneous treatment effects. Both machine learning (Lamont et al., 2018; Taddy et al., 2016) and optimization (Bertsimas et al., 2018) approaches are applied. Due to the difficulties of obtaining RCT datasets, observational studies become an alternative. Removing confounding is a core issue in causal inference with observational data. Confounding bias, selection bias and missing data are three main problems for causal inference with observational data. Some research estimates population causal effects with an instrumental variable (Bareinboim and Pearl, 2012); some research uses latent variable models to simultaneously discover hidden confounders and estimate causal effects (Louizos et al., 2017), which is robust against hidden confounding; some research focus on the recoverability in the presence of selection bias (Correa et al., 2019). In this paper, we assume that all the studied variables can be measured, which satisfies the strong ignorability assumption (Rosenbaum and Rubin, 1983).

In this branch, one of the core issues to deal with is mismatch between treatment and control groups. From the view of balancing, there are three ways. The first and classical way of balancing is referred to as matching (Ho et al., 2011): a control group is selected in order to maximize the similarity between the empirical covariate distributions in the treatment and control group. Mahalanobis distance and propensity score matching methods are proposed for population causal effect inference (Rubin, 2001; Diamond and Sekhon, 2013). An information theory-driven approach is proposed by using mutual information as the similarity measure (Sun and Nikolaev, 2016). In the second way of balancing, the inverse propensity score (IPS) method is proposed based on the variants of importance sampling (Sugiyama et al., 2007; Jiang and Li, 2016). The IPS is used to reweigh each unit sample to learn the counterfactuals, which is

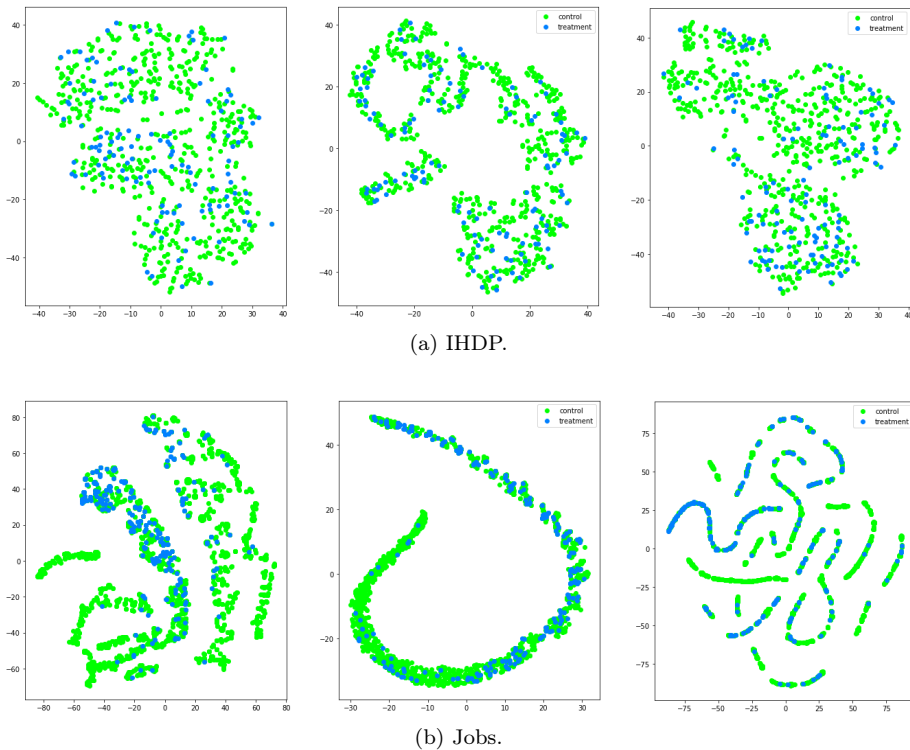


Figure 7: t-SNE visualization of treatment and control group, on the IHDP and Jobs datasets. The blue dots are treated units, and the green dots are control units. The left figures are the units in original covariate space, the middle figures are representations learned by ABCEI, and the right figures are representations learned by CFR-Wass; notice how the latter has control unit clusters unbalanced by treatment observations.

akin to counterfactual learning from logged bandit feedback (Swaminathan and Joachims, 2015b,a). In the third way, methods from representation learning are used to transform covariates from the original space into a latent representation space (Li and Fu, 2017). The representations are used as the input of predictors for individual and population causal effect inference. One study reported on use of a single neural network with the concatenation of representations and treatment variable as the input (Johansson et al., 2016). Separate models were trained for different treatments associated with a probabilistic integral metric to bound the generalization errors in (Shalit et al., 2017). Hard samples to preserve local similarity during balancing process were used in (Yao et al., 2018). Our methods are most similar to these third-way methods. The main difference between ABCEI and the existing approaches is that except balancing, we address the information loss problem by simultaneously estimating and maximizing the mutual information between latent representations and the input covariates.

From the technical viewpoint, our method lies into the field of representation learning. The main aim of learning representations is to obtain useful information from original data for downstream tasks like building predictors or classifiers. From principal components analysis (PCA) (Smith, 2002) to autoencoders (Vincent et al., 2008), many approaches account for learning representations. A proper way to evaluate the quality of learned representations is to measure the reconstruction error (Kingma and Welling, 2013). Specifically, reconstruction error is shown to be minimized by maximizing mutual information between input and the learned representations when their joint distributions for the encoder and decoder are matched (Belghazi et al., 2018). As a consequence, maximizing mutual information minimizes the information loss and the expected reconstruction error. We adopt this approach to regularize the encoder to preserve useful information for prediction tasks. However, in continuous and high-dimensional spaces, accurately computing MI is quite difficult. KL-divergence (Donsker and Varadhan, 1983) and Jensen-Shannon-divergence (JSD) (Nowozin et al., 2016) based methods are introduced for approximating mutual information with neural networks. We follow this way to build the neural network estimator for MI estimation.

More and more machine learning methods are employed for causal inference. For instance, Bayesian additive regression trees and Random forests were employed to estimate causal effects in (Sparapani et al., 2016) and (Wager and Athey, 2017) respectively. Some research discusses how domain adaptation (Daume III and Marcu, 2006) and generative adversarial networks (GAN) (Goodfellow, 2016) can be used for causal inference by generating balanced weights for unit samples (Ozery-Flato et al., 2018; Kuang et al., 2018). Fitting a model only with observed factual data by using the GAN framework, which is suitable for any number of treatments was proposed in (Yoon et al., 2018). The main difference between ABCEI and those methods is that we use adversarial learning to balance distributions of treatment group and control group in the latent representation space.

ABCEI does not need prior knowledge about treatment assignment. By following the design of Wasserstein GAN (Gulrajani et al., 2017), our adversarial balancing can make the encoder generate more similar distributions for treatment and control group. Another advantage of our method is that we account for the information loss problem by using a mutual information estimator to regularize the encoder. The mutual information estimator uses a neural network to simultaneously approximate and minimize the information loss, which persuades the encoder to learn representations preserving highly predictive information. Based on those advantages, the two components – mutual information estimator and adversarial balancing – combined together allow us to find the proper predictor for causal effect inference.



## 6 Conclusions

We propose a novel model for causal effect inference with observational data, called *ABCEI*, which is built on deep representation learning methods. *ABCEI* focuses on balancing latent representations from treatment and control groups by designing a two-player adversarial game. We use a discriminator to distinguish the representations from different groups. By adjusting the encoder parameters, our aim is to find an encoder that can fool the discriminator, which ensures that the distributions of treatment and control representations are as similar as possible. Our balancing method does not make any assumption on the form of the treatment selection function. With the mutual information estimator, we preserve highly predictive information from the original covariate space to latent space. Experimental results on benchmark datasets and synthetic datasets demonstrate that *ABCEI* is able to achieve robust, and substantially better performance than the state of the art.

In future work, we will explore more connections between relevant methods in domain adaptation (Daume III and Marcu, 2006) and counterfactual learning (Swaminathan and Joachims, 2015b) with the methods in causal inference. A proper extension would be to consider multiple treatment assignments or the existence of hidden confounders.

## References

- Abadi M, Barham P, Chen J, Chen Z, Davis A, Dean J, Devin M, Ghemawat S, Irving G, Isard M, et al. (2016) Tensorflow: a system for large-scale machine learning. In: OSDI, vol 16, pp 265–283
- Almond D, Chay KY, Lee DS (2005) The costs of low birth weight. *The Quarterly Journal of Economics* 120(3):1031–1083
- Bareinboim E, Pearl J (2012) Controlling selection bias in causal inference. In: *Artificial Intelligence and Statistics*, pp 100–108
- Belghazi MI, Baratin A, Rajeshwar S, Ozair S, Bengio Y, Courville A, Hjelm D (2018) Mutual information neural estimation. In: *Proceedings of the 35th International Conference on Machine Learning*, PMLR, vol 80, pp 531–540
- Bertsimas D, Korolko N, Weinstein A (2018) Identifying exceptional responders in randomized trials: An optimization approach. *INFORMS Journal on Optimization*, under review
- Breiman L (2001) Random forests. *Machine learning* 45(1):5–32
- Casucci S, Lin L, Hewner S, Nikolaev A (2017) Estimating the causal effects of chronic disease combinations on 30-day hospital readmissions based on observational medicaid data. *Journal of the American Medical Informatics Association* 25(6):670–678

- Clevert DA, Unterthiner T, Hochreiter S (2015) Fast and accurate deep network learning by exponential linear units (elus). arXiv preprint arXiv:151107289
- Correa JD, Tian J, Bareinboim E (2019) Identification of causal effects in the presence of selection bias. In: Proceedings of the 33rd AAAI Conference on Artificial Intelligence (AAAI)
- Crump RK, Hotz VJ, Imbens GW, Mitnik OA (2008) Nonparametric tests for treatment effect heterogeneity. *The Review of Economics and Statistics* 90(3):389–405
- Daume III H, Marcu D (2006) Domain adaptation for statistical classifiers. *Journal of artificial Intelligence research* 26:101–126
- Dehejia RH, Wahba S (2002) Propensity score-matching methods for nonexperimental causal studies. *Review of Economics and statistics* 84(1):151–161
- Diamond A, Sekhon JS (2013) Genetic matching for estimating causal effects: A general multivariate matching method for achieving balance in observational studies. *Review of Economics and Statistics* 95(3):932–945
- Donsker MD, Varadhan SS (1983) Asymptotic evaluation of certain markov process expectations for large time. iv. *Communications on Pure and Applied Mathematics* 36(2):183–212
- Dorie V (2016) Npci: Non-parametrics for causal inference
- Dorie V, Hill J, Shalit U, Scott M, Cervone D, et al. (2019) Automated versus do-it-yourself methods for causal inference: Lessons learned from a data analysis competition. *Statistical Science* 34(1):43–68
- Goodfellow I (2016) Nips 2016 tutorial: Generative adversarial networks. arXiv preprint arXiv:170100160
- Goodfellow I, Pouget-Abadie J, Mirza M, Xu B, Warde-Farley D, Ozair S, Courville A, Bengio Y (2014) Generative adversarial nets. In: *Advances in neural information processing systems*, pp 2672–2680
- Gulrajani I, Ahmed F, Arjovsky M, Dumoulin V, Courville AC (2017) Improved training of wasserstein gans. In: *Advances in Neural Information Processing Systems*, pp 5767–5777
- Hill JL (2011) Bayesian nonparametric modeling for causal inference. *Journal of Computational and Graphical Statistics* 20(1):217–240
- Hjelm RD, Fedorov A, Lavoie-Marchildon S, Grewal K, Trischler A, Bengio Y (2018) Learning deep representations by mutual information estimation and maximization. arXiv preprint arXiv:180806670

- Ho DE, Imai K, King G, Stuart EA, et al. (2011) Matchit: nonparametric preprocessing for parametric causal inference. *Journal of Statistical Software* 42(8):1–28
- Imai K, Ratkovic M (2014) Covariate balancing propensity score. *Journal of the Royal Statistical Society: Series B (Statistical Methodology)* 76(1):243–263
- Jiang N, Li L (2016) Doubly robust off-policy value evaluation for reinforcement learning. In: *Proceedings of the 33rd International Conference on International Conference on Machine Learning-Volume 48*, JMLR. org, pp 652–661
- Johansson F, Shalit U, Sontag D (2016) Learning representations for counterfactual inference. In: *International Conference on Machine Learning*, pp 3020–3029
- Kallus N (2018a) Balanced policy evaluation and learning. In: *Advances in Neural Information Processing Systems*, pp 8908–8919
- Kallus N (2018b) Deepmatch: Balancing deep covariate representations for causal inference using adversarial training. *arXiv preprint arXiv:180205664*
- Kingma DP, Ba J (2014) Adam: A method for stochastic optimization. *arXiv preprint arXiv:1412.6980*
- Kingma DP, Welling M (2013) Auto-encoding variational bayes. *arXiv preprint arXiv:1312.6114*
- Kinney JB, Atwal GS (2014) Equitability, mutual information, and the maximal information coefficient. *Proceedings of the National Academy of Sciences* 201309933
- Kuang K, Cui P, Athey S, Xiong R, Li B (2018) Stable prediction across unknown environments. In: *Proceedings of the 24th ACM SIGKDD International Conference on Knowledge Discovery & Data Mining*, ACM, pp 1617–1626
- Künzel SR, Sekhon JS, Bickel PJ, Yu B (2019) Metalearners for estimating heterogeneous treatment effects using machine learning. *Proceedings of the National Academy of Sciences* 116(10):4156–4165
- LaLonde RJ (1986) Evaluating the econometric evaluations of training programs with experimental data. *The American economic review* pp 604–620
- Lamont A, Lyons MD, Jaki T, Stuart E, Feaster DJ, Tharmaratnam K, Oberski D, Ishwaran H, Wilson DK, Van Horn ML (2018) Identification of predicted individual treatment effects in randomized clinical trials. *Statistical methods in medical research* 27(1):142–157
- Li S, Fu Y (2017) Matching on balanced nonlinear representations for treatment effects estimation. In: *Advances in Neural Information Processing Systems*, pp 929–939

- Louizos C, Shalit U, Mooij JM, Sontag D, Zemel R, Welling M (2017) Causal effect inference with deep latent-variable models. In: *Advances in Neural Information Processing Systems*, pp 6446–6456
- Lu M, Sadiq S, Feaster DJ, Ishwaran H (2018) Estimating individual treatment effect in observational data using random forest methods. *Journal of Computational and Graphical Statistics* 27(1):209–219
- Mooij JM, Peters J, Janzing D, Zscheischler J, Schölkopf B (2016) Distinguishing cause from effect using observational data: methods and benchmarks. *The Journal of Machine Learning Research* 17(1):1103–1204
- Morgan SL, Harding DJ (2006) Matching estimators of causal effects: Prospects and pitfalls in theory and practice. *Sociological methods & research* 35(1):3–60
- Ning Y, Peng S, Imai K (2018) Robust estimation of causal effects via high-dimensional covariate balancing propensity score. *arXiv preprint arXiv:181208683*
- Nowozin S, Cseke B, Tomioka R (2016) f-gan: Training generative neural samplers using variational divergence minimization. In: *Advances in Neural Information Processing Systems*, pp 271–279
- Ozery-Flato M, Thodoroff P, El-Hay T (2018) Adversarial balancing for causal inference. *arXiv preprint arXiv:181007406*
- Pearl J (2009) *Causality*. Cambridge university press
- Pearl J (2017) Detecting latent heterogeneity. *Sociological Methods & Research* 46(3):370–389
- Rosenbaum PR, Rubin DB (1983) The central role of the propensity score in observational studies for causal effects. *Biometrika* 70(1):41–55
- Rubin DB (2001) Using propensity scores to help design observational studies: application to the tobacco litigation. *Health Services and Outcomes Research Methodology* 2(3-4):169–188
- Rubin DB (2005) Causal inference using potential outcomes: Design, modeling, decisions. *Journal of the American Statistical Association* 100(469):322–331
- Shalit U, Johansson FD, Sontag D (2017) Estimating individual treatment effect: generalization bounds and algorithms. In: *Proceedings of the 34th International Conference on Machine Learning-Volume 70, JMLR. org*, pp 3076–3085
- Smith JA, Todd PE (2005) Does matching overcome lalonde’s critique of nonexperimental estimators? *Journal of econometrics* 125(1-2):305–353
- Smith LI (2002) A tutorial on principal components analysis. *Tech. rep.*

- Sparapani RA, Logan BR, McCulloch RE, Laud PW (2016) Nonparametric survival analysis using bayesian additive regression trees (bart). *Statistics in medicine* 35(16):2741–2753
- Sugiyama M, Krauledat M, MÄzller KR (2007) Covariate shift adaptation by importance weighted cross validation. *Journal of Machine Learning Research* 8(May):985–1005
- Sun L, Nikolaev AG (2016) Mutual information based matching for causal inference with observational data. *The Journal of Machine Learning Research* 17(1):6990–7020
- Swaminathan A, Joachims T (2015a) Batch learning from logged bandit feedback through counterfactual risk minimization. *Journal of Machine Learning Research* 16(1):1731–1755
- Swaminathan A, Joachims T (2015b) Counterfactual risk minimization: Learning from logged bandit feedback. In: *International Conference on Machine Learning*, pp 814–823
- Taddy M, Gardner M, Chen L, Draper D (2016) A nonparametric bayesian analysis of heterogenous treatment effects in digital experimentation. *Journal of Business & Economic Statistics* 34(4):661–672
- Vincent P, Larochelle H, Bengio Y, Manzagol PA (2008) Extracting and composing robust features with denoising autoencoders. In: *Proceedings of the 25th international conference on Machine learning*, pp 1096–1103
- Wager S, Athey S (2017) Estimation and inference of heterogeneous treatment effects using random forests. *Journal of the American Statistical Association*
- Yao L, Li S, Li Y, Huai M, Gao J, Zhang A (2018) Representation learning for treatment effect estimation from observational data. In: *Advances in Neural Information Processing Systems*, pp 2634–2644
- Yoon J, Jordon J, van der Schaar M (2018) Ganite: Estimation of individualized treatment effects using generative adversarial nets
- Zhao S, Heffernan N (2017) Estimating individual treatment effects from educational studies with residual counterfactual networks. In: *10th International Conference on Educational Data Mining*

## A Implementation details

The implementation of our method is based on Python and Tensorflow (Abadi et al., 2016).

All the experiments in this paper are conducted on a cluster with 1x Intel Xeon E5 2.2GHz CPU, 4x Nvidia Tesla V100 GPU and 256GB RAM.

## A.1 Training details

We adopt ELU (Clevert et al., 2015) as the non-linear activation function if there is no specification. We employ various numbers of fully-connected hidden layers with various sizes across networks: four layers with size 200 for the encoder network; two layers with size 200 for the mutual information estimator network; three layers with size 200 for the discriminator network; and finally, three layers with size 100 for the predictor network, following the structure of TARnet (Shalit et al., 2017). The gradient penalty weight  $\beta$  is set to 10.0, and the regularization weight is set to 0.0001.

In the training step, firstly we minimize  $L_{\Phi\Omega}$  by simultaneously optimizing  $\Phi$  and  $\Omega$  with one-step gradient descent. Then the representations  $h$  are passed to the discriminator to minimize  $L_D$  by optimizing  $D$  with 3-step gradient descent, in order to find a stable discriminator. Next, we use discriminator  $D$  to train encoder  $\Phi$  by minimizing  $L_\Phi$  with one-step gradient descent. Finally, encoder  $\Phi$  and predictor  $\Psi$  are optimized simultaneously by minimizing  $L_{\Phi\Psi}$ .

## A.2 Hyper-parameter optimization

Due to the reason that we cannot observe counterfactuals in observational datasets, standard cross-validation methods are not feasible. We follow the hyper-parameter optimization criterion in (Shalit et al., 2017), with an early stopping with regard to the lower bound on the validation set. Detail search space of hyper-parameter is demonstrated in Table 3. The optimal hyper-parameter settings for each benchmark dataset is demonstrated in Table 4.

## A.3 Computational complexity

Assuming the size of mini-batch is  $n$ , number of epochs is  $m$ , the computational complexity of our model is  $\mathcal{O}(n * m * ((\Phi_h - 1)\Phi_w^2 + (\Omega_h - 1)\Omega_w^2 + (D_h - 1)D_w^2 + (\Psi_h - 1)\Psi_w^2))$ . Here  $\Phi_h, \Omega_h, D_h, \Psi_h$  indicates the number of layers and  $\Phi_w, \Omega_w, D_w, \Psi_w$  indicates number of neurons in each layer in Neural Network  $\Phi, \Omega, D, \Psi$ .

# B Proofs

## B.1 Donsker-Varadhan

**Theorem 2 (Donsker-Varadhan)** *Let  $P, Q, G$  be distributions on the same support  $\mathcal{Z}$ , and let  $\mathcal{C}$  denote a family of functions  $\Omega : \mathcal{Z} \rightarrow \mathbb{R}$ , we have*

$$D_{KL}(P||Q) = \sup_{\Omega \in \mathcal{C}} \mathbb{E}_P[\Omega(Z)] - \log \mathbb{E}_Q [e^{\Omega(Z)}]$$

**Proof 1** *Given a fixed function  $\Omega$ , we can define distribution  $G$  by:*

$$dG = \frac{e^{\Omega(Z)}dQ}{\int_{\mathcal{Z}} e^{\Omega(Z)}dQ}$$

Equivalently, we have:

$$dG = e^{(\Omega(Z)-S)}dQ, \quad S = \log \mathbb{E}_Q \left[ e^{\Omega(Z)} \right]$$

Then by construction, we have:

$$\begin{aligned} & \mathbb{E}_P[\Omega(Z)] - \log \mathbb{E}_Q \left[ e^{\Omega(Z)} \right] \\ &= \mathbb{E}_P[\Omega(Z)] - S \\ &= \mathbb{E}_P \left[ \log \frac{dG}{dQ} \right] \\ &= \mathbb{E}_P \left[ \log \frac{dP dG}{dQ dP} \right] \\ &= \mathbb{E}_P \left[ \log \frac{dP}{dQ} - \log \frac{dP}{dG} \right] \\ &= D_{KL}(P||Q) - D_{KL}(P||G) \\ &\leq D_{KL}(P||Q) \end{aligned}$$

When distribution  $G$  is equal to  $P$ , this bound is tight.

Table 1: In-sample and out-of-sample results with mean and standard errors on the IHDP and Jobs dataset (lower = better).

Methods	IHDP			
	In-sample		Out-sample	
	$\sqrt{\epsilon_{PEHE}}$	$\epsilon_{ATE}$	$\sqrt{\epsilon_{PEHE}}$	$\epsilon_{ATE}$
OLS/ $LR_1$	5.8 $\pm$ .3	.73 $\pm$ .04	5.8 $\pm$ .3	.94 $\pm$ .06
OLS/ $LR_2$	2.4 $\pm$ .1	.14 $\pm$ .01	2.5 $\pm$ .1	.31 $\pm$ .02
BLR	5.8 $\pm$ .3	.72 $\pm$ .04	5.8 $\pm$ .3	.93 $\pm$ .05
BART	2.1 $\pm$ .1	.23 $\pm$ .01	2.3 $\pm$ .1	.34 $\pm$ .02
k-NN	2.1 $\pm$ .1	.14 $\pm$ .01	4.1 $\pm$ .2	.79 $\pm$ .05
RF	4.2 $\pm$ .2	.73 $\pm$ .05	6.6 $\pm$ .3	.96 $\pm$ .06
CF	3.8 $\pm$ .2	.18 $\pm$ .01	3.8 $\pm$ .2	.40 $\pm$ .03
BNN	2.2 $\pm$ .1	.37 $\pm$ .03	2.1 $\pm$ .1	.42 $\pm$ .03
TARNet	.88 $\pm$ .0	.26 $\pm$ .01	.95 $\pm$ .0	.28 $\pm$ .01
CFR-Wass	.71 $\pm$ .0	.25 $\pm$ .01	.76 $\pm$ .0	.27 $\pm$ .01
CEVAE	2.7 $\pm$ .1	.34 $\pm$ .01	2.6 $\pm$ .1	.46 $\pm$ .02
SITE	<b>.69 <math>\pm</math> .0</b>	.22 $\pm$ .01	.75 $\pm$ .0	.24 $\pm$ .01
ABCEI*	.74 $\pm$ .0	.12 $\pm$ .01	.78 $\pm$ .0	.11 $\pm$ .01
ABCEI**	.81 $\pm$ .1	.18 $\pm$ .03	.89 $\pm$ .1	.16 $\pm$ .02
ABCEI	.71 $\pm$ .0	<b>.09 <math>\pm</math> .01</b>	<b>.73 <math>\pm</math> .0</b>	<b>.09 <math>\pm</math> .01</b>
Methods	Jobs			
	In-sample		Out-sample	
	$R_{pol}$	$\epsilon_{ATT}$	$R_{pol}$	$\epsilon_{ATT}$
OLS/ $LR_1$	.22 $\pm$ .0	<b>.01 <math>\pm</math> .00</b>	.23 $\pm$ .0	.08 $\pm$ .04
OLS/ $LR_2$	.21 $\pm$ .0	.01 $\pm$ .01	.24 $\pm$ .0	.08 $\pm$ .03
BLR	.22 $\pm$ .0	.01 $\pm$ .01	.25 $\pm$ .0	.08 $\pm$ .03
BART	.23 $\pm$ .0	.02 $\pm$ .00	.25 $\pm$ .0	.08 $\pm$ .03
k-NN	.23 $\pm$ .0	.02 $\pm$ .01	.26 $\pm$ .0	.13 $\pm$ .05
RF	.23 $\pm$ .0	.03 $\pm$ .01	.28 $\pm$ .0	.09 $\pm$ .04
CF	.19 $\pm$ .0	.03 $\pm$ .01	.20 $\pm$ .0	.07 $\pm$ .03
BNN	.20 $\pm$ .0	.04 $\pm$ .01	.24 $\pm$ .0	.09 $\pm$ .04
TARNet	.17 $\pm$ .0	.05 $\pm$ .02	.21 $\pm$ .0	.11 $\pm$ .04
CFR-Wass	.17 $\pm$ .0	.04 $\pm$ .01	.21 $\pm$ .0	.08 $\pm$ .03
CEVAE	.15 $\pm$ .0	.02 $\pm$ .01	.26 $\pm$ .1	.03 $\pm$ .01
SITE	.17 $\pm$ .0	.04 $\pm$ .01	.21 $\pm$ .0	.09 $\pm$ .03
ABCEI*	.14 $\pm$ .0	.04 $\pm$ .01	.18 $\pm$ .0	.04 $\pm$ .01
ABCEI**	.15 $\pm$ .0	.05 $\pm$ .01	.19 $\pm$ .0	.04 $\pm$ .01
ABCEI	<b>.13 <math>\pm</math> .0</b>	.02 $\pm$ .01	<b>.17 <math>\pm</math> .0</b>	<b>.03 <math>\pm</math> .01</b>



Table 2: In-sample and out-of-sample results with mean and standard errors on the Twins dataset (AUC: higher = better,  $\epsilon_{ATE}$ : lower = better).

Methods	In-sample		Out-sample	
	$AUC$	$\epsilon_{ATE}$	$AUC$	$\epsilon_{ATE}$
OLS/ $LR_1$	.660 $\pm$ .005	.004 $\pm$ .003	.500 $\pm$ .028	.007 $\pm$ .006
OLS/ $LR_2$	.660 $\pm$ .004	.004 $\pm$ .003	.500 $\pm$ .016	.007 $\pm$ .006
BLR	.611 $\pm$ .009	.006 $\pm$ .004	.510 $\pm$ .018	.033 $\pm$ .009
BART	.506 $\pm$ .014	.121 $\pm$ .024	.500 $\pm$ .011	.127 $\pm$ .024
k-NN	.609 $\pm$ .010	.003 $\pm$ .002	.492 $\pm$ .012	.005 $\pm$ .004
BNN	.690 $\pm$ .008	.006 $\pm$ .003	.676 $\pm$ .008	.020 $\pm$ .007
TARNet	.849 $\pm$ .002	.011 $\pm$ .002	.840 $\pm$ .006	.015 $\pm$ .002
CFR-Wass	.850 $\pm$ .002	.011 $\pm$ .002	.842 $\pm$ .005	.028 $\pm$ .003
CEVAE	.845 $\pm$ .003	.022 $\pm$ .002	.841 $\pm$ .004	.032 $\pm$ .003
SITE	.862 $\pm$ .002	.016 $\pm$ .001	.853 $\pm$ .006	.020 $\pm$ .002
ABCEI*	.861 $\pm$ .001	.005 $\pm$ .001	.851 $\pm$ .001	.006 $\pm$ .001
ABCEI**	.855 $\pm$ .001	.005 $\pm$ .001	.849 $\pm$ .001	.006 $\pm$ .001
ABCEI	<b>.871 <math>\pm</math> .001</b>	<b>.003 <math>\pm</math> .001</b>	<b>.863 <math>\pm</math> .001</b>	<b>.005 <math>\pm</math> .001</b>

Table 3: Search space of hyper-parameter

Hyper-parameter	Range
$\lambda$	1e-3, 1e-4, 5e-5
$\beta$	1.0, 5.0, 10.0, 15.0
Optimizer	RMSProp, Adam
Depth of encoder layers	1, 2, 3, 4, 5, 6
Depth of discriminator layers	1, 2, 3, 4, 5, 6
Depth of predictor layers	1, 2, 3, 4, 5, 6
Dimension of encoder layers	50, 100, 200, 300, 500
Dimension of discriminator layers	50, 100, 200, 300, 500
Dimension of MI estimator layers	50, 100, 200, 300, 500
Dimension of predictor layers	50, 100, 200, 300, 500
Batch size	65, 80, 100, 200, 300, 500

Table 4: Optimal hyper-parameter for each benchmark dataset

Hyper-parameters	Datasets			
	IHDP	Jobs	Twins	ACIC
$\lambda$	$1e-4$	$1e-4$	$1e-4$	$1e-4$
$\beta$	10.0	10.0	10.0	10.0
Optimizer	Adam	Adam	Adam	Adam
Depth of encoder layers	4	5	5	4
Depth of discriminator layers	3	3	3	3
Depth of predictor layers	3	3	3	3
Dimension of encoder layers	200	200	300	200
Dimension of discriminator layers	200	200	200	200
Dimension of MI estimator layers	200	200	200	200
Dimension of predictor layers	100	100	200	100
Batch size	65	100	300	100